Scientia Iranica B (2013) 20(4), 1202–1212

SCIENTIA IRANICA

Sharif University of Technology
Scientia Iranica
Transactions B: Mechanical Engineering
www.scientiairanica.com

Exergy analysis of the triple effect parallel flow water-lithium bromide absorption chiller with three condensers

S. Sedigh and H. Saffari*

LNG Research Laboratory, School of Mechanical Engineering, Iran University of Science and Technology (IUST), Tehran, P.O. Box 16846, Iran.

Received 20 August 2011; received in revised form 5 November 2012; accepted 21 April 2013

KEYWORDS
Absorption Chiller;
Triple effect;
Water/lithium bromide;
Coefficient of performance;
Exergy;
Thermodynamic analysis.

Abstract. This paper is devoted to the thermodynamic analysis and investigation of the triple effect parallel flow water/lithium bromide chiller with three condensers. For this purpose, the conservation equations governing the cycle are written and the cycle is investigated regarding the first and second laws of thermodynamics. Next, the thermodynamic states of various points of the cycle, cycle efficiency, work and heat transfer, and also the exergy loss in various components of the cycle, are evaluated. Finally, the exergy analysis is carried out and the effect of effective parameters on the cycle's better performance has been studied. It was concluded that when the temperature of the high-temperature generator increases, the cycle COP increases and total exergy losses decrease, though the increase in COP and decrease in energy loss become negligible for temperatures higher than 210°C. Therefore, further temperature increase does not particularly contribute to an increase in COP or reduction of exergy losses, and this temperature is the most optimal temperature at which both COP and exergy losses have acceptable values.

1. Introduction

The environmental background of human beings has a direct influence on their mental state, physical situation, and working condition. Since, nowadays the majority of human life is spent inside, providing favourable environmental conditions within buildings is of crucial importance. Nowadays, with the increase of migration to large cities, the ventilation industry has also developed. A central cooling source in buildings includes chillers, which are used to cool the water required for ventilation systems, and in which the absorption systems of water-lithium bromide are widely used.

With the increasing demand for energy and its restrictions on availability, optimization routines of energy consumption have been considered and an essential change in energy consumption patterns has been taken into account. Because of the high price of electric energy generation, its replacement by heating energy will be widespread. This replacement has been achieved in absorption chillers, as their input energy is heat. Compression chillers use carbon-felour-celour refrigerants, which are destructive to the ozone layer [1], as opposed to absorption chillers, which do not use these substances. Apart from these advantages, due to lack of a compressor, absorption chillers have less moving and spinning parts, thus, lower noise and vibration, and, consequently, a higher useful lifetime. However, these systems have some disadvantages, such as the low coefficient of performance, crystallization, and corrosion etc., which have attracted the interest of some investigators.

*. *Corresponding author. Tel: +982177491228*
E-mail addresses: saeed_sedigh@yahoo.com (S. Sedigh) and saffari@iust.ac.ir (H. Saffari)

The single effect water-lithium bromide cycle has been analyzed based on the first law of thermodynamics [2], second law of thermodynamics [3] and exergy [4,5]. Lee and Sherif analysed the single effect cycle for cooling and heating applications [6], Liao et al. focused on combined heat and power generation applications [7], and Ayou et al. focused on combined absorption power and cooling cycles [8]. Similar analysis has also been investigated for a double effect water-lithium bromide cycle [9-11]. Garousi Farshi et al. analysed the exergy of double effect systems economically [12], while others have compared the performances of single and double effect cycles based on the first and second laws of thermodynamics [13-15].

Manole and Lage analyzed and optimized the triple effect series flow water/lithium bromide absorption cycle with one condenser [16]. The efficiency increase obtained using triple effect absorption cycles have theoretically been proven and some triple effect cycles have been patented, though few have industrial and commercial potential.

Triple effect technology is currently under active development by several of the leading absorption equipment manufacturers. The aim of the triple effect is to raise the gas-fired cooling COP to the range of 1.4 to 1.5 with only a modest increase in initial cost. Since these systems have not yet reached the market, the true potential of triple effect absorption technology has not been well defined. Triple effect inherently implies higher temperatures. The thermodynamic basis of the higher COP values comes from the increased availability of the high temperature heat input. The higher temperature causes significant increases in the corrosion rates for traditional materials of construction. Thus, most triple effect concepts revolve around the solution of the high temperature corrosion challenge.

Thermodynamic analysis of the triple effect water/lithium bromide absorption cycle with one condenser has been carried out [17-19], and Gomri compared the performances of the single, double and triple effect absorption cycles [20]. Moreover, some references considered optimization of the water/lithium bromide absorption cycles [21,22]. The analyses mentioned are static analysis of the water/lithium bromide absorption cycles, and some references have dynamically analyzed these systems [23-25]. The experimental test results in this field are very limited and sometimes inaccessible [26-28]. On the other hand, the price of various performance tests of the designed set-up is very high. Therefore, the significance of alternative experimental tests, such as numerical analysis, is revealed.

Almost all references have investigated absorption chillers with one condenser. Sedigh and Saffari analyzed a series and parallel flow water/lithium bromide double effect absorption system with two condensers [29], and this paper investigates a parallel flow triple effect water/lithium bromide absorption chiller with three condensers, based on the first and second laws of thermodynamics. Thermodynamic properties, heat transfer rates, the exergy destructed in the various components of the system, and the coefficient of performance, have been calculated. Finally, the exergy analysis is carried out and represented in diagrams to study the effect of effective parameters on the cycle's better performance.

2. The triple effect parallel flow water/lithium bromide absorption chiller with three condensers

Figure 1 shows a schematic illustration of the analyzed system. As can be seen, the system contains three generators, an absorber, three condensers an evaporator, three pumps, three expansion valves, and three Solution Heat Exchangers (SHE). The system has seven temperature levels (LTG, MTG, HTG, HTC, MTC, condenser and absorber) and four pressure levels (low pressure in the evaporator and absorber, medium pressure in the condenser and the LTG, medium pressure in the MTG and MTC, and high pressure in the HTG and HTC). The first generation works by external heat input at high temperature generation (HTG). This

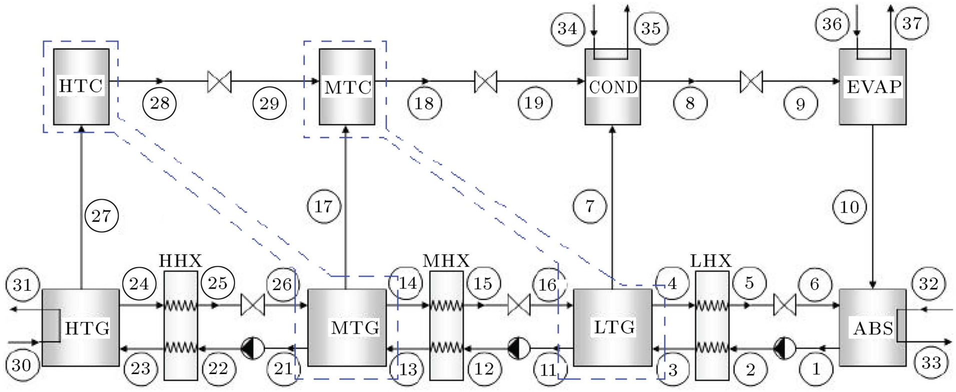

Figure 1. Triple effect parallel flow water/lithium bromide absorption chiller with three condensers.

cycle includes two internal heat exchange processes between a condenser and a generator. The second and third generations work by internal heat exchange at Medium Temperature Generation (MTG) and Low Temperature Generation (LTG), respectively. Thus, each unit of heat is used in three different generators to generate vapor, hence the name, triple effect. This particular cycle is a three-stage machine.

As shown in Figure 1, the vapor refrigerant coming from the evaporator (10) is absorbed by a liquid solution (6). This liquid solution is then pumped through the solution heat exchanger (LHX) (1-2-3) to LTG. The weak solution is boiled out by an intermediate strong solution coming from MTG, and the produced vapor goes to the condenser (7). The intermediate weak solution is then pumped through the solution heat exchanger (MHX) (11–12-13) to MTG, where it is boiled out by the strong solution coming from the HTG. In the next step, the liquid solution passes the pump and HHX (21-23), sent to the HTG and heated by an external heat input. The produced vapor is sent to the HTC and the strong solution comes back to the MTG. The vapor passes the HTG and, after cooling, enters the expansion valve as saturation liquid, where it exits as a two phase fluid (28-29). The two phase fluid enters the MTC, from where it is mixed with exit vapor. The two phase water exits MTC as a saturated liquid at MTC temperature. The same process occurs in the condenser and, finally, the saturated liquid passes the expansion valve (8-9), enters the evaporator and produces the required cooling capacity.

3. Assumptions and input parameters

In order to simulate the triple effect absorption refrigeration system, several assumptions are made, including the following:

1. The analysis is made under steady conditions.
2. The refrigerant (water) at the outlet of the condenser is saturated liquid.
3. The refrigerant (water) at the outlet of the evaporator is saturated vapor.
4. The Lithium bromide solution at the absorber outlet is a strong solution and is at absorber temperature.
5. The outlet temperatures from the absorber and generators correspond to equilibrium conditions of mixing and separation, respectively.
6. Pressure losses in the pipelines and all heat exchangers are negligible.
7. Heat exchange between the system and surroundings, other than that prescribed by heat transfer at the HPG, evaporator, condenser and absorber, does not occur.
8. The referenced environmental state for the system is water at an environmental temperature, T_0, of 25°C and 1 atmospheric pressure (P_0).
9. The system produces chilled water.

The system rejects heat to cool the water at the condenser and absorber.

Fixed data used in the simulation are summarized in Table 1.

Investigation of this cycle requires some working and fixed parameters. These parameters, given in Table 1, are obtained from [20] and include the following: Required cooling load, Q_{ev}, efficiency of heat exchangers, E_{ff}, condenser temperature, T_{cd}, absorber temperature, T_{ab}, evaporator temperature, T_{ev}, high-pressure generator temperature, T_{gh}, temperature of inlet water to absorber, temperature of outlet water from condenser, temperatures of inlet and outlet water to and from evaporator, and temperature of inlet steam to high temperature generator.

Table 1. Fixed data used in the simulation.

Fixed data	Symbol	Amount	
Refrigeration capacity	Q_{ev}	300	(kW)
Heat exchanger effectiveness	Eff	70	%
Condensation temperature	T_{cd}	35	(°C)
Absorber temperature	T_{ab}	35	(°C)
Evaporator temperature	T_{ev}	8	(°C)
HTG temperature	T_{gh}	180	(°C)
Inlet temperature of cooling water to absorber	T_{32}	27	(°C)
Outlet temperature of cooling water from condenser	T_{35}	32	(°C)
Inlet temperature of chilled water	T_{36}	11	(°C)
Outlet temperature of chilled water	T_{37}	16	(°C)
Inlet temperature of hot water	T_{30}	200	(°C)

When heat exchanger effectiveness increases, the COP of the cycle increases. The reason is that if heat exchanger effectiveness is higher, less heat is lost from the system and, therefore, the COP of the cycle is higher. Here, however, heat exchanger effectiveness is considered constant and equal to 70% according to [20].

4. Thermodynamic analysis

4.1. Mass conservation

The mass conservation law for each component is written as:

$$\sum \dot{m}_i = \sum \dot{m}_o. \tag{1}$$

4.2. Conservation of concentration

The law of concentration conservation for each component is written as:

$$\sum \dot{m}_i X_i = \sum \dot{m}_o X_o. \tag{2}$$

4.3. Analysis of the first law of thermodynamics for the system

The first law of thermodynamics yields the energy balance of each component of the absorption system as follows (each component can be treated as a control volume with inlet and outlet streams, heat transfer and work interaction):

$$\left(\sum \dot{m}_i h_i - \sum \dot{m}_o h_o\right) + \left(\sum Q_i - \sum Q_o\right) + W = 0. \tag{3}$$

The energy balance equations for some of the components of the single effect system are expressed as follows:

LHX:

$$Eff_{\text{LHX}} = \frac{T_4 - T_5}{T_4 - T_2}, \tag{4}$$

$$Q_{\text{LHX}} = \dot{m}_1.(h_3 - h_2), \tag{5}$$

$$Q_{\text{LHX}} = \dot{m}_4.(h_4 - h_5). \tag{6}$$

MHX:

$$Eff_{\text{MHX}} = \frac{T_{14} - T_{15}}{T_{14} - T_{12}}, \tag{7}$$

$$Q_{\text{MHX}} = \dot{m}_{11}.(h_{13} - h_{12}), \tag{8}$$

$$Q_{\text{MHX}} = \dot{m}_{14}.(h_{14} - h_{15}). \tag{9}$$

HHX:

$$Eff_{\text{HHX}} = \frac{T_{24} - T_{25}}{T_{24} - T_{22}}, \tag{10}$$

$$Q_{\text{HHX}} = \dot{m}_{21}.(h_{23} - h_{22}), \tag{11}$$

$$Q_{\text{HHX}} = \dot{m}_{24}.(h_{24} - h_{25}). \tag{12}$$

HTC:

$$Q_{\text{HTC}} = \dot{m}_{27}.h_{27} - \dot{m}_{28}.h_{28}. \tag{13}$$

MTC:

$$Q_{\text{MTC}} = \dot{m}_{17}.h_{17} - \dot{m}_{18}.h_{18} + \dot{m}_{29}.h_{29}. \tag{14}$$

Condenser:

$$Q_{cd} = \dot{m}_7.h_7 + \dot{m}_{19}.h_{19} - \dot{m}_8.h_8), \tag{15}$$

$$Q_{cd} = \dot{m}_{34}.cp(T_{35} - T_{34}). \tag{16}$$

HTG:

$$Q_{gh} = \dot{m}_{27}h_{27} + \dot{m}_{24}h_{24} - \dot{m}_{23}h_{23}, \tag{17}$$

$$Q_{gh} = \dot{m}_{30}.cp(T_{30} - T_{31}). \tag{18}$$

MTG:

$$0 = Q_{gm} + \dot{m}_{13}h_{13} + \dot{m}_{26}h_{26} - \dot{m}_{14}h_{14} - \dot{m}_{21}h_{21} - \dot{m}_{17}h_{17}, \tag{19}$$

$$Q_{\text{HTC}} = Q_{gm}. \tag{20}$$

LTG:

$$0 = Q_{gl} + \dot{m}_3h_3 + \dot{m}_{16}h_{16} - \dot{m}_4h_4 - \dot{m}_{11}h_{11} - \dot{m}_7h_7, \tag{21}$$

$$Q_{\text{MTC}} = Q_{gl}. \tag{22}$$

Evaporator:

$$Q_{ev} = \dot{m}_9.(h_{10} - h_9), \tag{23}$$

$$Q_{ev} = \dot{m}_{36}.cp(T_{36} - T_{37}). \tag{24}$$

Absorber:

$$\dot{m}_{10}h_{10} + \dot{m}_6h_6 - Q_{ab} - \dot{m}_1h_1 = 0, \tag{25}$$

$$Q_{ab} = \dot{m}_{32}.cp(T_{33} - T_{32}). \tag{26}$$

4.4. Analysis of the system exergy

Many researchers report that the best method for evaluation of a process is the exergy analysis [4,5]. Exergy is the maximum work that a flow or a system can do when it goes from the present state to the state of equilibrium with its surroundings. The exergy analysis of a system is a combination of the first and second laws of thermodynamics, and is defined as the maximum work that a system or flow can do when it is in equilibrium with special conditions. Analysis of the system exergy is as follows:

$$\sum \dot{m}_i e_i - \sum \dot{m}_o e_o + \dot{Q}\left(1 - \frac{T_o}{T}\right) - \dot{W} - \dot{E}_D = 0, \tag{27}$$

in which the first two terms are the sum of inlet exergy flow and outlet exergy flow. The third term is the heat exergy, where it is positive when the heat is transferred to the system. $\dot{W}$ is the mechanical work transferred to or from the system, and the last term, $\dot{E}_D$, is the exergy destroyed due to inside irreversibility. By neglecting the kinetic and potential energies and noting that the chemical exergy is zero, the specific exergy is defined as [15]:

$$ex = (h - h_0) - T_0(s - s_0). \quad (28)$$

And the exergy losses for each of the components of the system are written as:

$$\Delta E_{\text{HTC}} = \dot{m}_{27}e_{27} - \dot{m}_{28}e_{28}, \quad (29)$$

$$\Delta E_{\text{MTC}} = \dot{m}_{29}e_{29} + \dot{m}_{17}e_{17} - \dot{m}_{18}e_{18}, \quad (30)$$

$$\Delta E_{cd} = \dot{m}_{19}e_{19} + \dot{m}_{7}e_{7} + \dot{m}_{34}e_{34} - \dot{m}_{8}e_{8} - \dot{m}_{35}e_{35}, \quad (31)$$

$$\Delta E_{ev} = \dot{m}_{9}e_{9} + \dot{m}_{36}e_{36} - \dot{m}_{10}e_{10} - \dot{m}_{37}e_{37}, \quad (32)$$

$$\Delta E_{ab} = \dot{m}_{10}e_{10} + \dot{m}_{6}e_{6} + \dot{m}_{32}e_{32} - \dot{m}_{1}e_{1} - \dot{m}_{33}e_{33}, \quad (33)$$

$$\Delta E_{\text{LHX}} = \dot{m}_{4}e_{4} + \dot{m}_{2}e_{2} - \dot{m}_{5}e_{5} - \dot{m}_{3}e_{3}, \quad (34)$$

$$\Delta E_{\text{MHX}} = \dot{m}_{14}e_{14} + \dot{m}_{12}e_{12} - \dot{m}_{13}e_{13} - \dot{m}_{15}e_{15}, \quad (35)$$

$$\Delta E_{\text{HHX}} = \dot{m}_{24}e_{24} + \dot{m}_{22}e_{22} - \dot{m}_{23}e_{23} - \dot{m}_{25}e_{25}, \quad (36)$$

$$\Delta E_{gl} = \dot{m}_{16}e_{16} + \dot{m}_{3}e_{3} - \dot{m}_{4}e_{4} - \dot{m}_{11}e_{11} - \dot{m}_{7}e_{7}, \quad (37)$$

$$\Delta E_{gm} = \dot{m}_{26}e_{26} + \dot{m}_{13}e_{13} - \dot{m}_{14}e_{14} - \dot{m}_{21}e_{21} - \dot{m}_{17}e_{17}, \quad (38)$$

$$\Delta E_{gh} = \dot{m}_{23}e_{23} + \dot{m}_{30}e_{30} - \dot{m}_{24}e_{24} - \dot{m}_{31}e_{31} - \dot{m}_{27}e_{27}, \quad (39)$$

$$\Delta E_{P_1} = \dot{m}_{1}e_{1} - \dot{m}_{2}e_{2} + W_{P_1}, \quad (40)$$

$$\Delta E_{P_2} = \dot{m}_{11}e_{11} - \dot{m}_{12}e_{12} + W_{P_2}, \quad (41)$$

$$\Delta E_{\text{valve28}-29} = \dot{m}_{28}e_{28} - \dot{m}_{29}e_{29}, \quad (42)$$

$$\Delta E_{\text{valve18}-19} = \dot{m}_{18}e_{18} - \dot{m}_{19}e_{19}, \quad (43)$$

$$\Delta E_{\text{valve25}-26} = \dot{m}_{25}e_{25} - \dot{m}_{26}e_{26}, \quad (44)$$

$$\Delta E_{\text{valve15}-16} = \dot{m}_{15}e_{15} - \dot{m}_{16}e_{16}, \quad (45)$$

$$\Delta E_{\text{valve8}-9} = \dot{m}_{8}e_{8} - \dot{m}_{9}e_{9}, \quad (46)$$

$$\Delta E_{\text{valve5}-6} = \dot{m}_{5}e_{5} - \dot{m}_{6}e_{6}. \quad (47)$$

5. Results and discussion

A code has been written for analysis of the system. First, the analysis of the first law of thermodynamics has been investigated for each of the system components, and then, having obtained the properties of all points of the system, the second law analysis has been carried out on different system components. Tables 2, 3 and 4 show the simulation results for the

Table 2. Thermodynamic properties of each state point.

State point	T (°C)	$\dot{m}$ (kg/s)	h (kJ/kg)	s (kJ/kg K)
1	35.0	1.889	79.5	0.231
2	35.0	1.889	79.5	0.231
3	58.8	1.889	129.4	0.384
4	73.3	1.763	170.8	0.439
5	46.5	1.763	117.3	0.281
6	42.6	1.763	117.3	0.257
7	65.5	0.034	2622.1	8.530
8	35.0	0.127	146.6	0.505
9	8.0	0.127	146.6	0.523
10	8.0	0.127	2515.2	8.948
11	65.5	1.378	143.5	0.426
12	65.5	1.378	143.6	0.426
13	101.1	1.378	218.6	0.636
14	123.0	1.286	270.1	0.708
15	82.7	1.286	189.7	0.493
16	74.1	1.286	189.7	0.444
17	114.4	0.037	2711	7.827
18	78.3	0.092	327.7	1.055
19	35.0	0.092	327.7	1.093
21	114.4	0.824	246.7	0.710
22	114.5	0.824	246.8	0.711
23	155.0	0.824	332.6	0.924
24	180.0	0.769	384.3	0.983
25	134.1	0.769	292.4	0.764
26	78.6	0.769	292.4	0.470
27	170.5	0.055	2807.0	7.259
28	128.0	0.055	537.9	1.613
29	78.2	0.055	537.9	1.653
30	200.0	8.000	2792.5	6.431
31	194.7	8.000	828.8	2.281
32	27.0	14.000	113.1	0.395
33	33.4	14.000	139.8	0.483
34	30.3	14.000	126.8	0.440
35	32.0	14.000	134.0	0.464
36	16.0	14.286	67.1	0.239
37	11.0	14.286	46.2	0.166

Table 3. Transfer rates of each component.

Component	Amount	
Q_{absorber}	375.1	(kW)
$Q_{\text{evaporator}}$	300.0	(kW)
$Q_{\text{low temperature generator}}$	100.2	(kW)
$Q_{\text{medium temperature generator}}$	125.3	(kW)
$Q_{\text{high temperature generator}}$	176.5	(kW)
$Q_{\text{low temperature condenser}}$	101.5	(kW)
$Q_{\text{medium temperature condenser}}$	100.2	(kW)
$Q_{\text{high temperature condenser}}$	125.3	(kW)
$Q_{\text{low temperature heat exchanger}}$	94.2	(kW)
$Q_{\text{medium temperature heat exchanger}}$	103.5	(kW)
$Q_{\text{high temperature heat exchanger}}$	70.6	(kW)

thermodynamic properties, heat transfer rates of each component and the exergy destructed at the various components of the system, respectively.

The COP and amount of energy consumption by pumps are presented in Table 5.

The effect of variations in HTG temperature on the coefficient of performance of the system at various evaporator temperatures is shown in Figure 2. The operating condition changed here is the HTG temperature.

Figure 3 shows the variations of the coefficient of performance of single, double and series triple effect absorption refrigeration systems with generator temperatures at various evaporator temperatures taken from [15]. As can be seen from Figures 2 and 3, the variations and the range of COP are the same.

Here, the variations of the system Coefficient Of Performance (COP) are investigated in terms of the parameters considered fixed at the beginning. Figure 4 shows the variations of the Coefficient Of Performance (COP) with evaporator temperature. It can be seen

Table 5. COP and amount of energy consumption by pumps.

W pump 1	0.0055	(KW)
W pump 2	0.0342	(KW)
W pump 3	0.1132	(KW)
COP	1.7	—

Table 4. Exergy destructed at the various components of the system.

Exergy loss in absorber	1256	(KW)
Exergy loss in evaporator	29.82	(KW)
Exergy loss in low temperature generator	4.394	(KW)
Exergy loss in medium temperature generator	11.95	(KW)
Exergy loss in high temperature generator	5753	(KW)
Exergy loss in low temperature condenser	1.374	(KW)
Exergy loss in medium temperature condenser	16.71	(KW)
Exergy loss in high temperature condenser	34.52	(KW)
Exergy loss in low temperature heat xchanger	2.453	(KW)
Exergy loss in medium temperature heat exchanger	3.467	(KW)
Exergy loss in high temperature heat exchanger	1.646	(KW)
Exergy loss in pump 1	0.003354	(KW)
Exergy loss in pump 2	0.02429	(KW)
Exergy loss in pump 3	0.1058	(KW)
Exergy loss in valves	480.6	(KW)
Total exergy loss	7490	(KW)
Absorber pressure (P1)	1.073	(KPa)
Evaporator pressure (P1)	1.073	(KPa)
Low temperature generator pressure (P2)	5.627	(KPa)
Low temperature condenser pressure (P2)	5.627	(KPa)
Medium temperature generator pressure (P3)	44.145	(KPa)
Medium temperature condenser pressure (P3)	44.145	(KPa)
High temperature generator pressure (P4)	254.227	(KPa)
High temperature condenser pressure (P4)	254.227	(KPa)

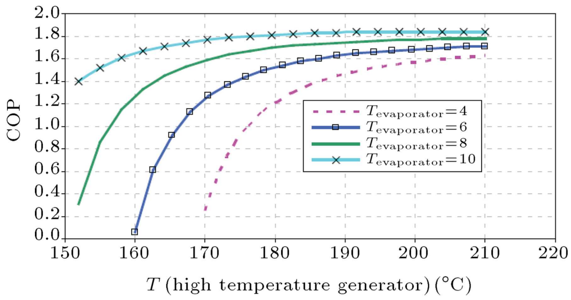

Figure 2. Variation of coefficient of performance of the systems.

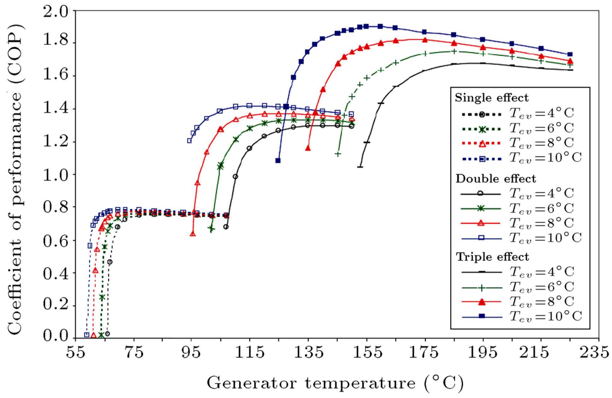

Figure 3. Variation of coefficient of performance of single and double effect absorption refrigeration systems [15].

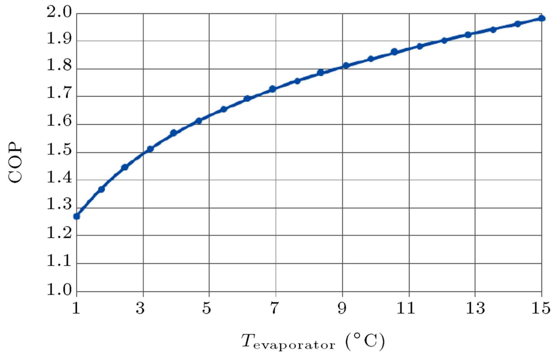

Figure 4. Variations of the Coefficient Of Performance (COP) with evaporator temperature.

that when the evaporator temperature increases, the result is an increase in COP.

Figure 5 shows the variations of the Coefficient Of Performance (COP) with condenser temperature.

As can be seen, the increase in condenser temperature causes a decrease in the cycle's COP. This is because the decrease in condenser temperature causes more heat release. Therefore, in an absorption cycle, the condenser temperature decrease is more favorable, due to the increase in COP.

Figure 6 shows the variations of the Coefficient Of Performance (COP) with the absorber temperature. It can be seen that the COP increases with an increase in absorber temperature.

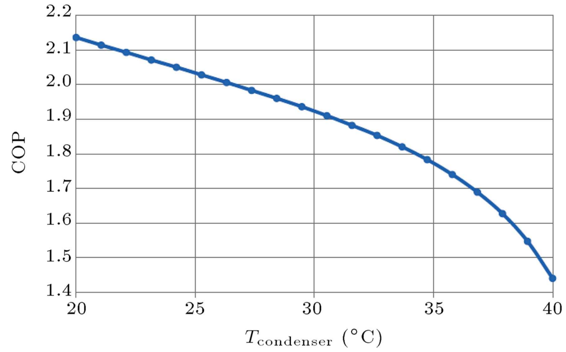

Figure 5. Variations of the Coefficient Of Performance (COP) with condenser temperature.

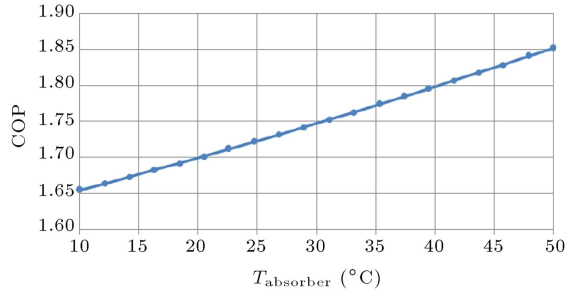

Figure 6. The variations of the Coefficient Of Performance (COP) with absorber temperature.

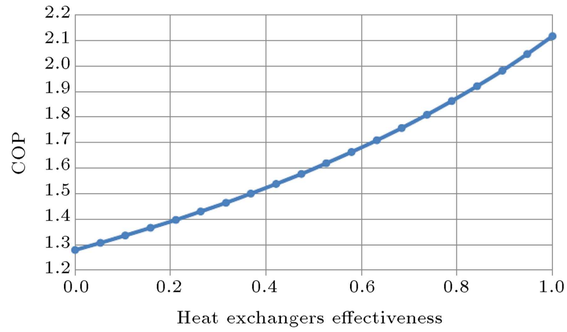

Figure 7. Variations of the Coefficient Of Performance (COP) with heat exchanger effectiveness.

It can be seen from Figure 7 that when the heat exchangers effectiveness increases, the cycle's COP increases. This is because the heat loss is lower in a heat exchanger with higher effectiveness, which results in the higher overall performance of the cycle.

Another parameter having significant influence on the performance of the absorption chillers is the lithium bromide solution mass flow rate in the absorption camber outlet. This value is controlled by the solution pump. Here, the effect of this parameter variation on COP is investigated. As can be seen from Figure 8, the chiller COP decreases with an increase in the solution mass flow rate.

Contrary to the variations of the COP with the solution mass flow rate, the chiller cooling load increases with the solution mass flow rate, shown in Figure 9.

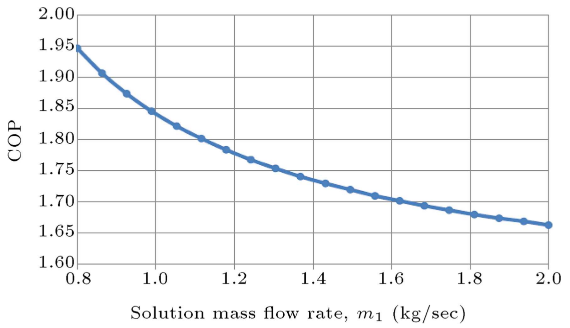

Figure 8. Variations of COP with the lithium bromide solution mass flow rate.

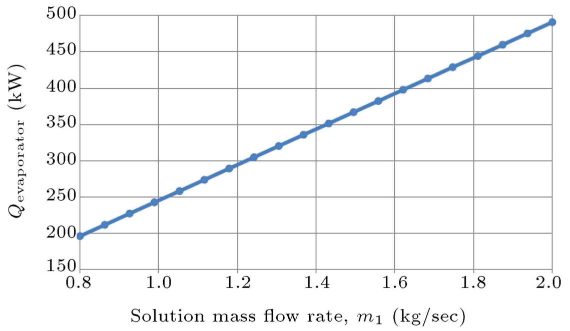

Figure 9. The variations of the cooling load with the water/lithium bromide solution mass flow rate.

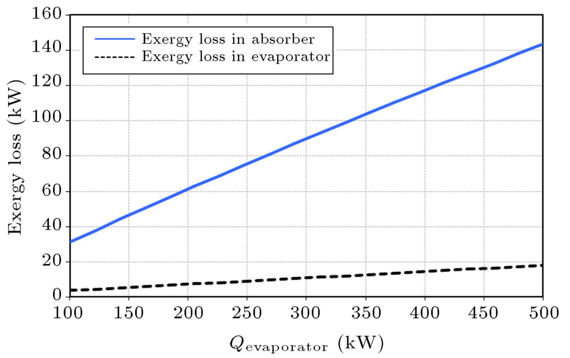

Figure 10. Variations of exergy losses in absorber and evaporator with evaporator capacity.

Here, the exergy loss in various cycle components is investigated in terms of the evaporator cooling load, which was fixed in the beginning.

Figure 10 shows the variations of exergy loss in the absorber and evaporator, in terms of the cooling load. As can be seen, the exergy losses in both the absorber and evaporator increase with the increase of cooling load. Also, the exergy loss in the absorber is much higher than that in the evaporator.

Figure 11 shows the variations of exergy loss in the condensers, in terms of the cooling load.

As expected, in all three condensers, when the condenser temperature increases, the exergy loss increases. The HTC has the highest value of exergy loss compared to the MTC and LTC.

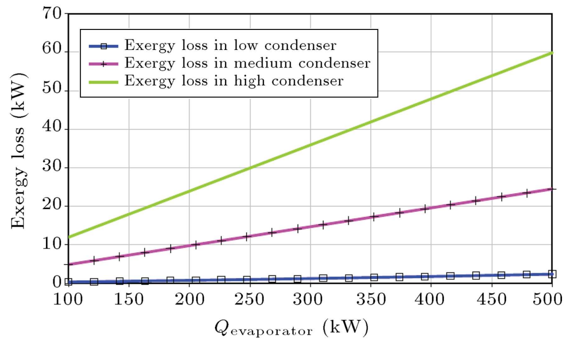

Figure 11. Variations of exergy loss in low, medium, and high temperature condensers with evaporator capacity.

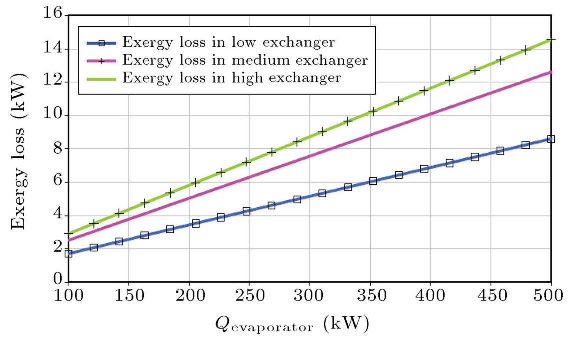

Figure 12. Variations of exergy loss in low, medium, and high temperature heat exchangers with evaporator capacity.

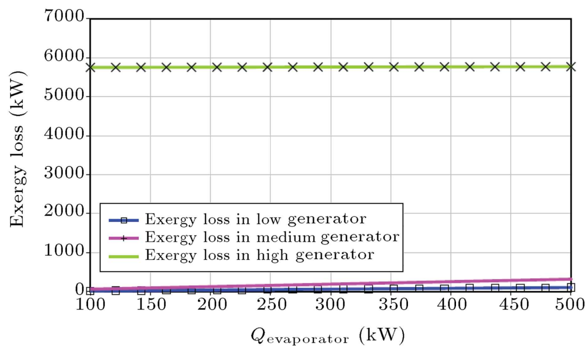

Figure 13. Variation of exergy loss in low, medium, and high temperature generators with variation of evaporator capacity.

The variations of exergy loss in the heat exchangers are shown in terms of the cooling load in Figure 12. As seen, the exergy losses in the heat exchangers also increase with an increase in the cooling load.

Figures 13 and 14 show the variations of exergy loss in the three generators, in terms of the cooling load. As expected, the exergy loss increases with an increase in generator temperature, such that the HTG has the highest exergy loss compared to MTG and LTG.

It can be seen that the exergy losses in the high temperature generator have very low dependency on the cooling load. However, according to Figure 14,

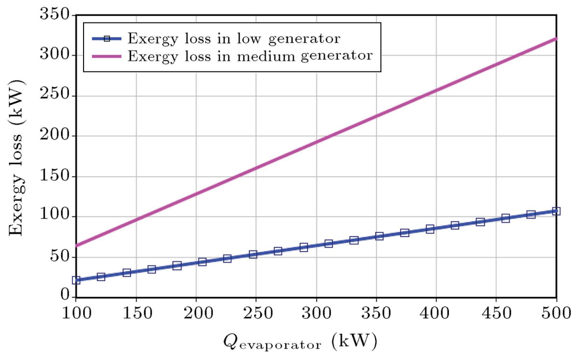

Figure 14. Variations of exergy loss in low and medium temperature generators with variation of evaporator capacity (clarification of Figure 13).

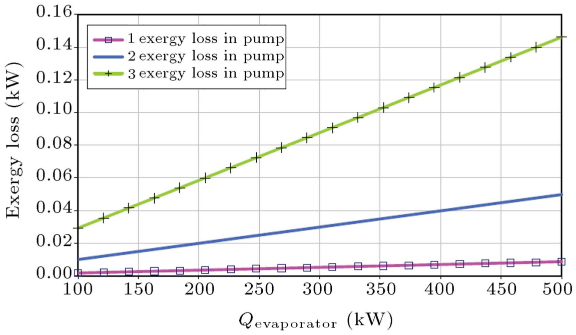

Figure 15. Variations of exergy loss in pump in terms of the heat exchange in evaporator.

the exergy losses in medium and low temperature generators have a dependency on the cooling load, in which exergy loss increases with an increase in cooling load.

Figure 15 shows the variations of exergy loss in the pumps, in terms of the heat exchange in the evaporator. As seen, in all three pumps, exergy losses increase with an increase in cooling load. However, exergy loss in the pumps is so low that it can be neglected.

Here, we seek to optimize the temperature for the high-temperature generator. Figure 16 shows the variations of total exergy losses and COP with the temperature of the high-temperature generator. As can be seen, the increase in temperature of the high-temperature generator results in an increase in the system COP, a decrease in the exergy loss of all system components and, therefore, the total exergy losses of the system. It should be mentioned that the COP increase and decrease in exergy loss in the high-temperature generator are negligible for temperatures higher than 210°C. Therefore, the most optimal temperature for the high-temperature generator is 210°C in which both COP and the exergy losses have acceptable values, and further temperature increase does not contribute considerably to an increase in COP or in the reduction of exergy losses.

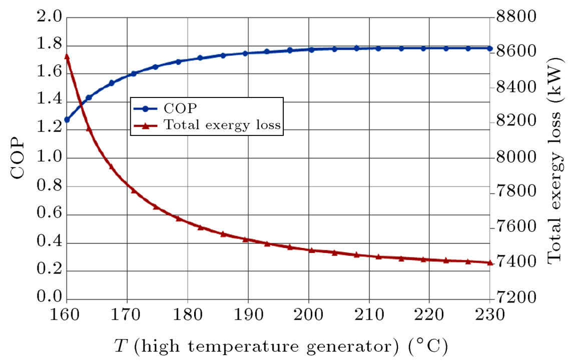

Figure 16. Variations of total exergy loss and COP with temperature of the high-temperature generator.

6. Conclusions

In this paper, the thermodynamic analysis of a triple effect parallel flow water/lithium bromide absorption chiller for cooling and heating applications is performed, and the exergy loss of each component is calculated. A computer program has been developed to predict its performance. It was revealed that by increasing the temperatures of the evaporator, condenser, absorber and HTG, the coefficient of performance is increased, and by decreasing the condenser temperature, the coefficient of performance is decreased. In addition, exergy loss is in proportion with the cooling capacity of the chiller and inversely in proportion with the generator temperature. The variations of various parameters, such as Coefficient Of Performance (COP), exergy losses in each component, and total exergy losses with the temperature of the high-temperature generator, are then plotted. Finally, it was concluded that when the temperature of the high-temperature generator increases, the cycle COP increases and total exergy losses decrease. However, the increase in COP and decrease in exergy loss become negligible for temperatures higher than 210°C. Therefore, further temperature increase does not contribute considerably to the increase in COP or to the reduction in exergy loss. Thus, this temperature is the most optimal temperature at which both the COP and exergy losses have acceptable values.

Nomenclature

A	Area (m^2)
COP	Coefficient Of Performance
Ex	Exergy per mass unit (kJ kg^{-1})
E	Exergy (kW)
Eff	Heat exchanger efficiency (%)
G	Gravitational acceleration (m s^{-2})
H	Specific enthalpy (kJ kg^{-1})
H	Total enthalpy (kJ)

HTG	High temperature generator
HTC	High temperature condenser
HHX	High temperature heat exchanger
LTG	Low temperature generator
LHX	Low temperature heat exchanger
MTG	Medium temperature generator
MTC	Medium temperature condenser
MHX	Medium temperature heat exchanger
M	Mass flow rate (kg s^{-1})
P	Pressure (kPa)
Q	Heat (kJ)
S	Specific entropy (kJ $kg^{-1}K^{-1}$)
S	Total entropy (kJ/K)
SHE	Solution heat exchanger
T	Temperature (K)
U	Specific internal energy (kJ/kg)
U	Total internal energy (kJ), Overall heat transfer coefficient (m^2K/kJ)
X	Concentration (%)
V	Volume (m^3)
W	Work (kJ)

Greek symbols

Δ	Exergy losses, difference
Ω	Humidity ratio
ϕ	Relative humidity

Subscripts

Ab	Absorber
D	Loss
I	Number of the flow branch, input, inlet
Irr	Irreversible
O	Output, outlet
Ev	Evaporator
Cd	Condenser
Gh	High Temperature Generator (HTG)
Gm	Medium Temperature Generator (MTG)
Gl	Low Temperature Generator (LTG)
HHX	High temperature heat exchanger
MHX	Medium temperature heat exchanger
LHX	Low temperature heat exchanger
HTC	High temperature condenser
MTC	Medium temperature condenser
P	Pump
0	Surroundings
V	Vapour
G	Gas
Gen	Generation

References

1. Chua, H.T., Toh, H.K., Malek, A.N.K. and Sirinivasan, K. "A general thermodynamic framework for understanding the behavior of absorption chillers", *International Journal of Refrigeration*, **23**, pp. 491-507 (2000).

2. Kim, D.S. and Infante Ferreira, C.A. "Analytic modeling of steady state single-effect absorption cycles", *International Journal of Refrigeration*, pp. 1012-1020 (2008).

3. Kilic, M. and Kaynakli, O. "Second law-based thermodynamic analysis of water-lithium bromide absorption refrigeration system", *Energy*, **32**, pp. 1505-1512 (2007).

4. Sencan, A., Yakut, K.A., Kalogirou, S.A. "Exergy analysis of lithium bromide/water absorption systems", *Renewable Energy*, **30**, pp. 645-657 (2005).

5. Misra, R.D., Sahoo, P.K. and Gupta, A. "Application of the exergetic cost theory to the LiBr/H2O vapour absorption system", *Energy*, **27**, pp. 1009-1025 (2002).

6. Lee, S.F. and Sherif, S.A. "Thermodynamic analysis of a lithium bromide/water absorption system for cooling and heating applications", *International Journal of Energy Research*, pp. 1019-1031 (2001).

7. Liao, X., Garland, P. and Radermacher, R. "The modeling of air-cooled absorption chiller integration in CHP system", *ASME International Mechanical Engineering Congress and Exposition*, November 13-20, Anaheim, California USA (2004).

8. Ayou, D., Bruno, J., Saravanan, R. and Coronas, A. "An overview of combined absorption power and cooling cycles", *Renewable and Sustainable Energy Reviews*, **21**, pp. 728-748 (2013).

9. Figueredo, G.R., Bourouis, M. and Coronas, A. "Thermodynamic modeling of a two-stage absorption chiller driven at two-temperature levels", *Applied Thermal Engineering*, **28**, pp. 211-217 (2008).

10. Gomri, R. and Hakimi, R. "Second law analysis of doubl-effect vapours absorption cooler system", *Energy Conversion and Management*, **49**, pp. 3343-3348 (2008).

11. Martinez, H. and Rivera, W. "Energy and exergy analysis of a double absorption heat transformer operating with water/lithium bromide", *International Journal of Energy Research*, pp. 662-674 (2009).

12. Garousi Farshi, L., Mahmoudi, S.M.S., Rosen, M.A., Yari, M. and Amidpour, M. "Exergoeconomic analysis of double effect absorption refrigeration systems", *Energy Conversion and Management*, **65**, pp. 13-25 (2013).

13. Kaushik, S.C. and Arora, A. "Energy and exergy analysis of single effect and series flow double effect

water-lithium bromide absorption refrigeration systems", *International Journal of Refrigeration*, **(32)**, pp. 1247-1258 (2009).

14. Arora, A. and Kaushik, S.C. "Theoretical analysis of $LiBr/H_2O$ absorption refrigeration systems", *International Journal of Energy Research*, pp. 1-20 (2009).

15. Gomri, R. "Investigation of the potential of application of single effect and multiple effect absorption cooling systems", *Conference of GCREEDER*, Amman-Jordan (2009).

16. Manole, D.M. and Lage, J.L. "Thermodynamic optimization method of a triple effect absorption system with wased heat recovery", *Heat Mass Transfer*, pp. 655-663 (1995).

17. Kaita, Y. "Simulation results of triple-effect absorption cycles", *International Journal of Refrigeration*, **25**, pp. 999-1007 (2002).

18. Kim, J.S., Ziegler, F. and Lee, H. "Simulation of the compressor-assisted triple-effect $H_2O/LiBr$ absorption cooling cycles", *Applied Thermal Engineering*, **22**, pp. 295-308 (2002).

19. Balkan, F., Colak, N. and Hepbasli, A. "Performance evaluation of a triple-effect evaporator with forward feed using exergy analysis", *International Journal of Energy Research*, pp. 455-470 (2005).

20. Gomri, R. "Second law comparison of single effect and double effect vapour absorption refrigeration systems", *Energy Conversion and Management*, **50**, pp. 1279-1287 (2009).

21. Kızılkan, Onder, Sencan, A., Kalogirou, S.A. "Thermoeconomic optimization of a LiBr absorption refrigeration system", *Chemical Engineering and Processing*, **46**, pp. 1376-1384 (2007).

22. Misra, R.D., Sahoo, P.K. and Gupta, A. "Thermoeconomic evaluation and optimization of a double-effect $H_2O/LiBr$ vapour-absorption refrigeration system", *International Journal of Refrigeration*, **28**, pp. 331-343 (2005).

23. Kohlenbach, P. and Ziegler, F. "A dynamic simulation model for transient absorption chiller performance Part I: Numerical results and experimental verification", *International Journal of Refrigeration*, pp. 1-9 (2007).

24. Shin, Y., Seo, J.A., Cho, H.W., Nam, S.C. and Jeong, J.H. "Simulation of dynamics and control of a double-effect $LiBr$-H_2O absorption chiller", *Applied Thermal Engineering*, **29**, pp. 2718-2725 (2009).

25. Evola, G., Le Pierrès, N., Boudehenn, F. and Papillon, P. " Proposal and validation of a model for the dynamic simulation of a solar-assisted single-stage LiBr/water absorption chiller", *International Journal of Refrigeration*, **36**, pp. 1015-1028 (2013).

26. Aphornratana, S. and Sriveerakul, T. "Experimental studies of a single-effect absorption refrigerator using aqueous lithium-bromide: Effect of operating condition to system performance", *Experimental Thermal and Fluid Science*, **32**, pp. 658-669 (2007).

27. Martinez, J. and Pinazo, J.M. "A method for design analysis of absorption machines", *International Journal of Refrigeration*, pp. 634-639 (2002).

28. Jayasekara, S. and Halgamuge, S. "Mathematical modeling and experimental verification of an absorption chiller including three dimensional temperature and concentration distributions", *Applied Energy*, **106**, pp. 232-242 (2013).

29. Sedigh, S. and Saffari, H. "Thermodynamic analysis of series and parallel flow water/lithium bromide double effect absorption system with two condensers", *Journal of Materials Science and Engineering*, **1**, pp. 1-9 (2011).

Biographies

Saeed Sedigh obtained a BS degree from Guilan University, Iran, and an MS degree from Iran University of Science and Technology, in Mechanical Engineering. His research interests include: thermodynamics, HVAC&R and systems energy efficiency.

Hamid Saffari is Associate Professor of Mechanical Engineering at Iran University of Science and Technology (IUST), Tehran, Iran. He has published many scientific papers in international journals, including the 'Journal of Energy and Buildings' and the 'Journal of Mechanical Science and Technology'. His research Interests include: boiling, condensation, two-phase flow, and HVAC&R.